

Research Article

Generalized Dynamic Switched Synchronization between Combinations of Fractional-Order Chaotic Systems

Wafaa S. Sayed,¹ Moheb M. R. Henein,¹ Salwa K. Abd-El-Hafiz,¹ and Ahmed G. Radwan^{1,2}

¹Engineering Mathematics and Physics Department, Faculty of Engineering, Cairo University, Giza 12613, Egypt

²Nanoelectronics Integrated Systems Center, Nile University, Cairo 12588, Egypt

Correspondence should be addressed to Ahmed G. Radwan; agradwan@ieee.org

Received 30 July 2016; Accepted 16 November 2016; Published 16 February 2017

Academic Editor: Michael Small

Copyright © 2017 Wafaa S. Sayed et al. This is an open access article distributed under the Creative Commons Attribution License, which permits unrestricted use, distribution, and reproduction in any medium, provided the original work is properly cited.

This paper proposes a novel generalized switched synchronization scheme among n fractional-order chaotic systems with various operating modes. Digital dynamic switches and dynamic scaling factors are employed, which offer many new capabilities. Dynamic switches determine the role of each system as a master or a slave. A system can either have a fixed role throughout the simulation time (static switching) or switch its role one or more times (dynamic switching). Dynamic scaling factors are used for each state variable of the master system. Such scaling factors control whether the master is a single system or a combination of several systems. In addition, these factors determine the generalized relation between the original systems from which the master system is built as well as the slave system(s). Moreover, they can be utilized to achieve different kinds of generalized synchronization relations for the purpose of generating new attractor diagrams. The paper presents a mathematical formulation and analysis of the proposed synchronization scheme. Furthermore, many numerical simulations are provided to demonstrate the successful generalized switched synchronization of several fractional-order chaotic systems. The proposed scheme provides various functions suitable for applications such as different master-slave communication models and secure communication systems.

1. Introduction

Chaos theory has always attracted the interest of scientific research because it has a wide spectrum of applications, such as in secure communication [1, 2], cryptography [3–8], circuit theory [9–12], and modeling multidisciplinary phenomena in physics, chemistry, and biology [13–15]. This is due to the fact that chaotic systems exhibit aperiodic, bounded, long-time evolution and sensitive dependence on initial conditions for some ranges of parameters. In the last few decades, the use of fractional calculus has flourished because of the advances in numerical methods for solving fractional-order systems and their implementations [16, 17]. It found its way to many applications including bioengineering [18], electromagnetics [19, 20], and image encryption [21]. Fractional-order chaotic systems with more parameters allow extra degrees of freedom and flexibility, which make them more suitable for a lot of applications compared to their integer-order counterparts.

Synchronization or coupling of two or more, identical or different, fractional-order chaotic systems has appeared a lot

in recent literature due to its applications in biological and physical systems, structural engineering, ecological models, secure communication, and cryptography [22–31]. Chaotic synchronization represents a challenge because chaotic systems are sensitive to initial conditions, where two trajectories starting at slightly different initial conditions exponentially diverge from each other in the long-term evolution. Many feedback control methods of synchronization have been used; yet, the active nonlinear control method [32–36] is utilized in this paper. Several papers handled conventional synchronization and antisynchronization of two identical chaotic systems starting at different initial conditions [32, 37] or two different systems [33]. Synchronized systems have exactly the same magnitude and phase while antisynchronized ones exhibit the same magnitude but opposite phase (180° phase shift). Generalized synchronization, in which the slave response could exhibit lower or higher amplitude than the master response via scaling or transformations, has also been discussed with applications to secure communication [38–40]. More recent researches focused on control and

synchronization in the fractional-order domain [24, 34, 41–44], introduced generalized synchronization with dynamic scaling suitable for chaotic modulation [35, 45], and provided the capability of control and switching for exchanging roles between master and slave systems [36, 46].

Meanwhile, master-slave communication has found its way to many applications such as industrial automation [47], groundwater remediation [48], and medical robotics and computer-assisted surgery [49]. Requirements on the number of devices and the type of interactions between them extend far beyond synchronization of two systems or one-to-one communication. For example, in one-to-many communication there is a single master and multiple slaves [50]. It might be the case that more than one device have the authority to communicate with the others or control their responses [51, 52]. Other examples include mutual interconnections [53] in which forward communication occurs from master to slave and backward communication occurs from slave to master. Role switching [54–56] is also presented for fairness and power management purposes. Recent research [57] investigated mutual synchronization of bidirectional coupling integer-order chaotic systems, which can be applied in full-duplex chaos-based communication.

In this paper, a novel synchronization scheme among n fractional-order chaotic systems is proposed. This generalized scheme offers different synchronization alternatives that can be utilized in many of the aforementioned applications. Each chaotic system can play the role of a master or a slave using switching control. The master can be a single system or a linear combination of two or more systems. Furthermore, different operational modes are possible using static or dynamic switches and scaling factors. For each of the proposed synchronization alternatives, numerical simulations are performed. The results of those simulations validate the presented mathematical analysis and demonstrate successful synchronization.

More specifically, factors that generate various synchronization cases include the following: the role of each system as a master or a slave and the generalized relation between the original systems from which the master system is built as well as the slave system(s). Each system can have a fixed role as master or slave throughout the simulation time, which is called static switching. In dynamic switching, a system can switch its role one or more times. In all the presented cases, the master system can be a single system or constructed as a combination of two or more systems. Such a combination can be their summation or difference or a linear combination of them. Different scaling factors, each corresponding to one state variable, are used for each system. In addition to their role as coefficients of the linear combination, they can be utilized to achieve different kinds of generalized synchronization relations for the time series of each state variable and, consequently, generate new attractor diagrams.

The rest of this paper is organized as follows. Section 2 reviews the numerical method utilized in solving fractional-order differential equations. The main chaotic properties of the systems selected for validating the proposed generalized synchronization scheme are briefly listed as well. Section 3 introduces the block diagram of the proposed scheme, the

theory behind it, and the associated mathematical analysis to compute the values of all required control signals in a generalized manner. Section 4 provides various numerical experiments that cover the main capabilities of the proposed synchronization scheme and successfully validate our mathematical analysis. Section 5 provides a discussion of the validity of the proposed analysis for various values of fractional orders with simulations. In addition, it suggests several applications for the proposed generalized dynamic switched synchronization. Finally, Section 6 summarizes the main contributions of the paper.

2. Numerical Solution and Properties of the Utilized Systems

This section presents a brief review of the numerical method used to solve fractional differential equations. It also summarizes the properties of the chaotic systems, which are selected for the simulations in Section 4.

2.1. Numerical Solution of a System of Fractional Differential Equations. Finding robust and stable numerical and analytical methods for solving a system of fractional differential equations has recently been an active research topic. The definition of Grünwald–Letnikov derivative has been used in numerical analysis to discretize fractional differential equations. The Caputo fractional derivative [16] of order α is defined as

$$D^\alpha f(t) = \frac{d^\alpha f(t)}{dt^\alpha} = \begin{cases} \frac{1}{\Gamma(m-\alpha)} \int_0^t \frac{f^m(\tau)}{(t-\tau)^{\alpha-m+1}} d\tau & m-1 < \alpha < m \\ \frac{d^m}{dt^m} f(t) & \alpha = m, \end{cases} \quad (1)$$

where m is the first integer greater than α and $\Gamma(\cdot)$ is the gamma function defined by

$$\Gamma(z) = \int_0^\infty e^{-t} t^{z-1} dt, \quad (2)$$

$$\Gamma(z+1) = z\Gamma(z).$$

For fractional-order chaotic systems, m is usually fixed to 1. Hence, $\alpha \in (0, 1]$.

Grünwald–Letnikov method of approximation [58] is defined as follows:

$$D^\alpha f(t) \approx h^{-\alpha} \sum_{j=0}^k (-1)^j \binom{\alpha}{j} f(t_{k-j}), \quad (3)$$

where h is the step size. Consider the fractional-order differential equation

$$D^\alpha y(t) = f(y(t), t). \quad (4)$$

Using (3), (4) can be discretized as follows:

$$y(t_k) = f(y(t_k), t_k) h^\alpha - \sum_{j=1}^k c_j^\alpha y(t_{k-j}), \quad (5)$$

where $t_k = kh$ and c_j^α are the Grünwald–Letnikov coefficients defined as

$$c_j^\alpha = \left(1 - \frac{1+\alpha}{j}\right) c_{j-1}^\alpha, \quad j = 1, 2, 3, \dots, \quad c_0^\alpha = 1. \quad (6)$$

The same algebraic manipulation can be applied to a system of three fractional-order differential equations:

$$D^\alpha x = f(x, y, z), \quad (7a)$$

$$D^\beta y = g(x, y, z), \quad (7b)$$

$$D^\gamma z = h(x, y, z), \quad (7c)$$

where $0 < \alpha, \beta, \gamma \leq 1$, to obtain the corresponding solutions. A comprehensive study of fractional differential equations can be found in [59], which includes mathematical analysis of the existence of the solution of such models and presents methods for finding it. Researches that propose novel fractional-order chaotic systems devote part of their studies to the existence and uniqueness of their solutions such as [26]. The well-posedness of more generalized and complicated models has been studied in the literature as well, for example, [60–62].

In the rest of this paper, a step size of 0.005 is employed according to the system properties and a total simulation time of 200 time units is used except where stated otherwise.

2.2. Properties of the Utilized Systems. Simulation results will be demonstrated through various examples and cases in Section 4 when the number of systems, n , equals 3. Three fractional-order chaotic systems with piecewise and quadratic nonlinearities were selected from [58]: Cellular Neural Networks-3 cells (CNN-3 cells), Liu, and Financial systems. These systems were first presented and studied in [63], [64], and [65], respectively. Table 1 shows the equations and strange attractors of the three systems for the specified values of parameters and initial conditions, which are marked in red. In addition, time series of the three state variables for the three systems are shown in Figure 1. Each system is designated a color that is fixed throughout the paper to distinguish its attractor diagram and time series. The values of parameters and initial conditions given in Table 1 are used in the simulations, which are presented in Section 4. More examples with different orders of fractional derivatives are presented in Section 5.

3. The Proposed Generalized Synchronization Scheme and Its Mathematical Analysis

Consider n communication sources for which the roles as master or slave are to be given during simulation. Each one is represented as a chaotic system, which consists of three

fractional-order differential equations. For instance, system j is given by

$$\begin{aligned} D^\alpha x_j &= f_j(x_j, y_j, z_j) + S_j u_{jx}, \\ D^\beta y_j &= g_j(x_j, y_j, z_j) + S_j u_{jy}, \\ D^\gamma z_j &= h_j(x_j, y_j, z_j) + S_j u_{jz}, \end{aligned} \quad (8)$$

for $j = 1, 2, \dots, n$, where $f_j(x_j, y_j, z_j)$ implicitly includes the system parameters. Figure 2 shows the block diagram of the proposed generalized switched synchronization scheme when the number of systems $n = 3$, where

S_1, S_2 , and S_3 are control switches for systems 1, 2, and 3, respectively, where $S_i \in \{0, 1\}$. S_i equals “0” when system i acts as a master and equals “1” when it acts as a slave.

k_{ix}, k_{iy} , and k_{iz} are real-valued scaling factors for the variables of system i when it acts as a master, where $i \in \{1, 2, 3\}$.

u_{ix}, u_{iy} , and u_{iz} are control functions corresponding to each state variable of system i using active nonlinear control synchronization technique, where $i \in \{1, 2, 3\}$.

If it is required for a certain system not to take place in the synchronization process, its control switch should be set to zero with zero scaling factors as well. Control signals can be calculated based on active nonlinear control technique and Lyapunov stability according to the mathematical analysis that will be explained. All synchronization alternatives, which are detailed in Section 4, are supported with various experiments and numerical simulations that validate the proposed scheme and conform to the presented mathematical analysis.

For the newly proposed n -system generalized dynamic switched synchronization, the generic steps to calculate the control signals depend on superposition. The control functions u_{ix}, u_{iy} , and u_{iz} , corresponding to system i , affect its response only when it acts as a slave. For each slave system i , the corresponding master system will be given by the general relations:

$$x_m = \sum_{j=1, j \neq i}^n k_{jx} (1 - S_j) x_j, \quad (9a)$$

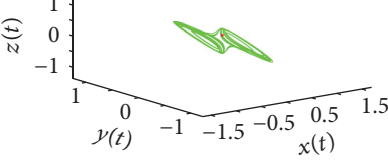
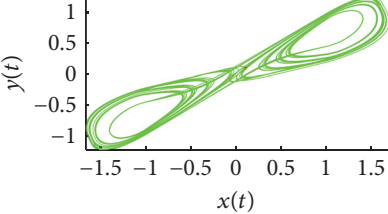
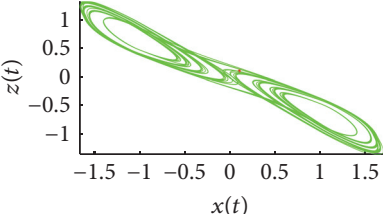
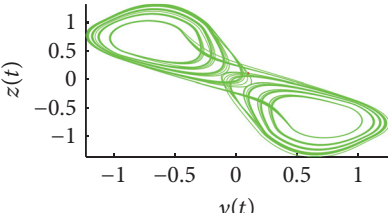
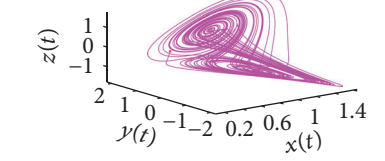
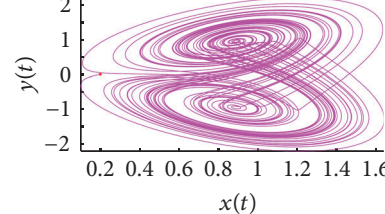
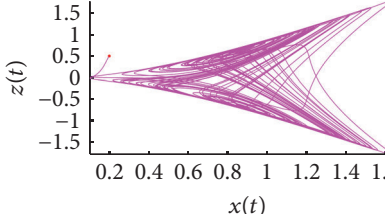
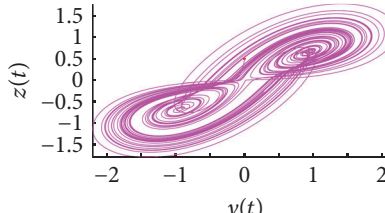
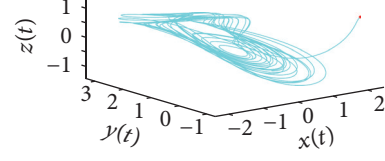
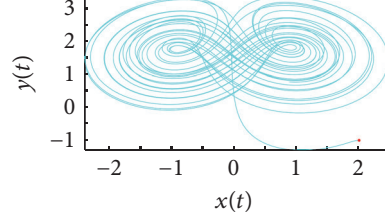
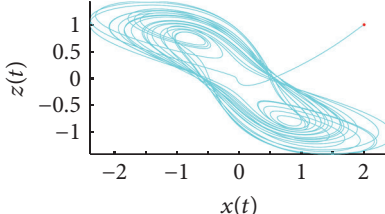
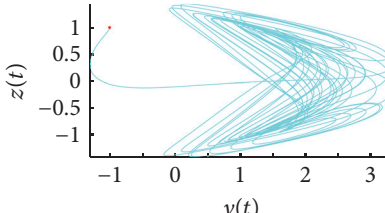
$$y_m = \sum_{j=1, j \neq i}^n k_{jy} (1 - S_j) y_j, \quad (9b)$$

$$z_m = \sum_{j=1, j \neq i}^n k_{jz} (1 - S_j) z_j, \quad (9c)$$

where the scaling factors k_{jx}, k_{jy} , and k_{jz} control the relation between the slave system i and the original response of the rest of the systems before the construction of the overall master combination. The error vector e_i is given by

$$e_i = \begin{pmatrix} e_{ix} \\ e_{iy} \\ e_{iz} \end{pmatrix} = \begin{pmatrix} x_i - x_m \\ y_i - y_m \\ z_i - z_m \end{pmatrix}. \quad (10)$$

TABLE 1: Equations, parameter values, initial conditions, and strange attractors of the utilized systems at $(\alpha, \beta, \gamma) = (0.99, 0.99, 0.99)$.

CNN-3 cells system	Liu system	Financial system
$D^\alpha x_1 = -x_1 + a_1 f(x_1) - g_1 f(y_1) - g_1 f(z_1) + S_1 u_{1x}$ $D^\beta y_1 = -y_1 - g_1 f(x_1) + b_1 f(y_1) - d_1 f(z_1) + S_1 u_{1y}$ $D^\gamma z_1 = -z_1 - g_1 f(x_1) + d_1 f(y_1) + c_1 f(z_1) + S_1 u_{1z}$ where $f(x) = 0.5(x+1 - x-1)$	$D^\alpha x_2 = -a_2 x_2 + d_2 y_2^2 + S_2 u_{2x}$ $D^\beta y_2 = b_2 y_2 - g_2 x_2 z_2 + S_2 u_{2y}$ $D^\gamma z_2 = -c_2 z_2 + f_2 x_2 y_2 + S_2 u_{2z}$	$D^\alpha x_3 = z_3 + (y_3 - a_3) x_3 + S_3 u_{3x}$ $D^\beta y_3 = 1 - b_3 y_3 - x_3^2 + S_3 u_{3y}$ $D^\gamma z_3 = -x_3 - c_3 z_3 + S_3 u_{3z}$
$(a_1, b_1, c_1, d_1, g_1) = (1.24, 1.1, 1, 4.4, 3.21)$	$(a_2, b_2, c_2, d_2, f_2, g_2) = (1, 2.5, 5, 1, 4, 4)$	$(a_3, b_3, c_3) = (1, 0.1, 1)$
$(x_{10}, y_{10}, z_{10}) = (0.1, 0.1, 0.1)$	$(x_{20}, y_{20}, z_{20}) = (0.2, 0, 0.5)$	$(x_{30}, y_{30}, z_{30}) = (2, -1, 1)$
   	   	   

Thus, the fractional derivatives of the error vector e_i are given as

$$\begin{pmatrix} D^\alpha e_{ix} \\ D^\beta e_{iy} \\ D^\gamma e_{iz} \end{pmatrix} = \begin{pmatrix} f_i(x_i, y_i, z_i) + S_i u_{ix} - \sum_{j=1, j \neq i}^n (k_{jx}(1-S_j) f_j(x_j, y_j, z_j) + k_{jx}(1-S_j) S_j u_{jx}) \\ g_i(x_i, y_i, z_i) + S_i u_{iy} - \sum_{j=1, j \neq i}^n (k_{jy}(1-S_j) g_j(x_j, y_j, z_j) + k_{jy}(1-S_j) S_j u_{jy}) \\ h_i(x_i, y_i, z_i) + S_i u_{iz} - \sum_{j=1, j \neq i}^n (k_{jz}(1-S_j) h_j(x_j, y_j, z_j) + k_{jz}(1-S_j) S_j u_{jz}) \end{pmatrix}. \quad (11)$$

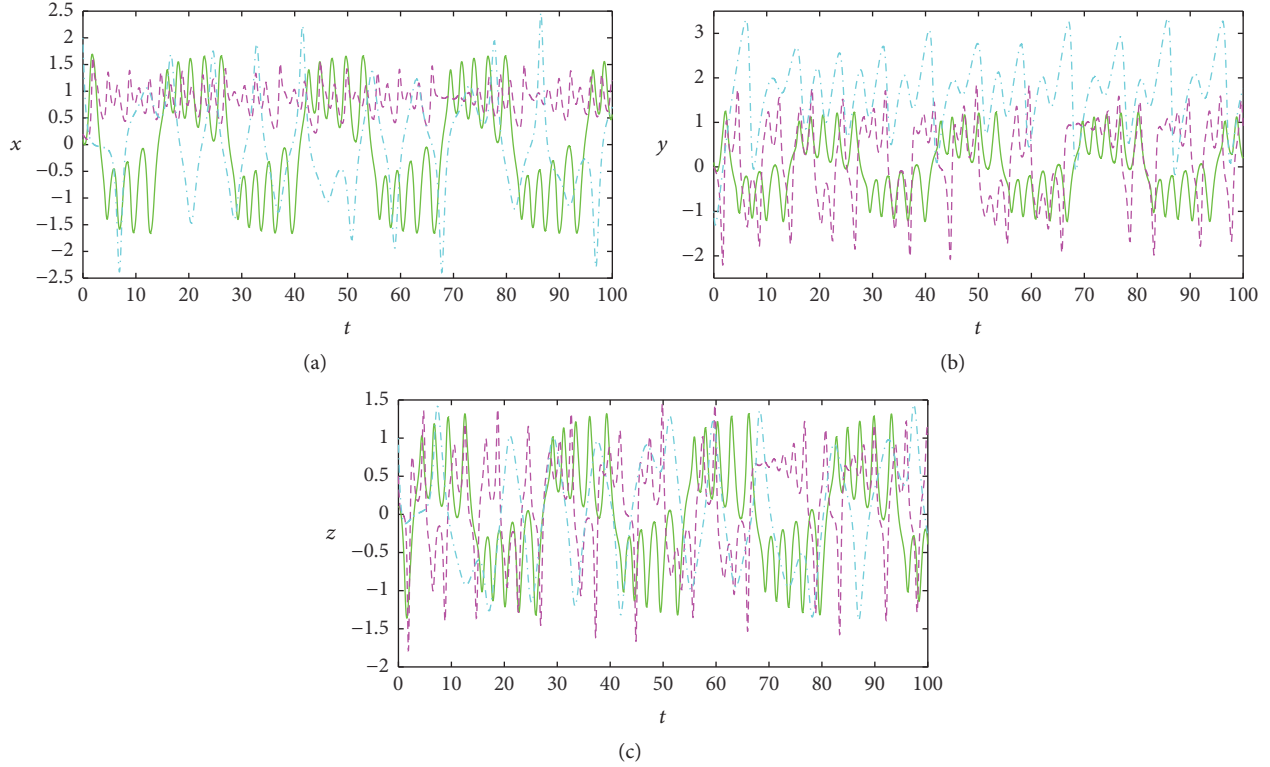


FIGURE 1: Time series of the three selected systems: (a) x time series, (b) y time series, and (c) z time series.

It should be noted that the terms $k_{jx}(1 - S_j)S_j u_{jx}$, $k_{jy}(1 - S_j)S_j u_{jy}$, and $k_{jz}(1 - S_j)S_j u_{jz}$ vanish because S_j is either zero or one.

Based on the nonlinear control theory and Lyapunov stability theory [32–36], these derivatives should be decaying functions of the error. Let

$$\begin{pmatrix} D^\alpha e_{ix} \\ D^\beta e_{iy} \\ D^\gamma e_{iz} \end{pmatrix} = \begin{pmatrix} V_{ix}(e_{ix}) \\ V_{iy}(e_{iy}) \\ V_{iz}(e_{iz}) \end{pmatrix}, \quad (12)$$

where the terms $V_{ix}(e_{ix})$, $V_{iy}(e_{iy})$, and $V_{iz}(e_{iz})$ form a system of linear equations in the errors e_{ix} , e_{iy} , and e_{iz} . These terms should be chosen carefully to force negative eigenvalues for the synchronization system and to form a stable system with zero steady state [66]. They usually take the form

$$\begin{pmatrix} V_{ix}(e_{ix}) \\ V_{iy}(e_{iy}) \\ V_{iz}(e_{iz}) \end{pmatrix} = \begin{pmatrix} -k_{ux} & 0 & 0 \\ 0 & -k_{uy} & 0 \\ 0 & 0 & -k_{uz} \end{pmatrix} \begin{pmatrix} e_{ix} \\ e_{iy} \\ e_{iz} \end{pmatrix}, \quad (13)$$

where $k_{ux}, k_{uy}, k_{uz} \geq 1$ are tuning parameters that control the error. There is a tradeoff between the value of the tuning parameters and the speed of achieving synchronization. In the rest of this paper, the value $k_{ux} = k_{uy} = k_{uz} = 50$ is

chosen. Therefore, for $1 \leq i \leq n$, substituting from (12) into (11) and setting $S_i = 1$ yield

$$u_{ix} = V_{ix}(e_{ix}) + \sum_{j=1, j \neq i}^n k_{jx}(1 - S_j) f_j(x_j, y_j, z_j) \quad (14a)$$

$$- f_i(x_i, y_i, z_i),$$

$$u_{iy} = V_{iy}(e_{iy}) + \sum_{j=1, j \neq i}^n k_{jy}(1 - S_j) g_j(x_j, y_j, z_j) \quad (14b)$$

$$- g_i(x_i, y_i, z_i),$$

$$u_{iz} = V_{iz}(e_{iz}) + \sum_{j=1, j \neq i}^n k_{jz}(1 - S_j) h_j(x_j, y_j, z_j) \quad (14c)$$

$$- h_i(x_i, y_i, z_i).$$

The obtained relations ((14a), (14b), and (14c)) are substituted in the equations of the systems from which our analysis started at the beginning of this section. This mathematical analysis and the obtained relations for the control signals are general and can be adapted to fit various cases. Section 4 presents the simulation results of such various cases through setting the values of the switches and scaling factors.

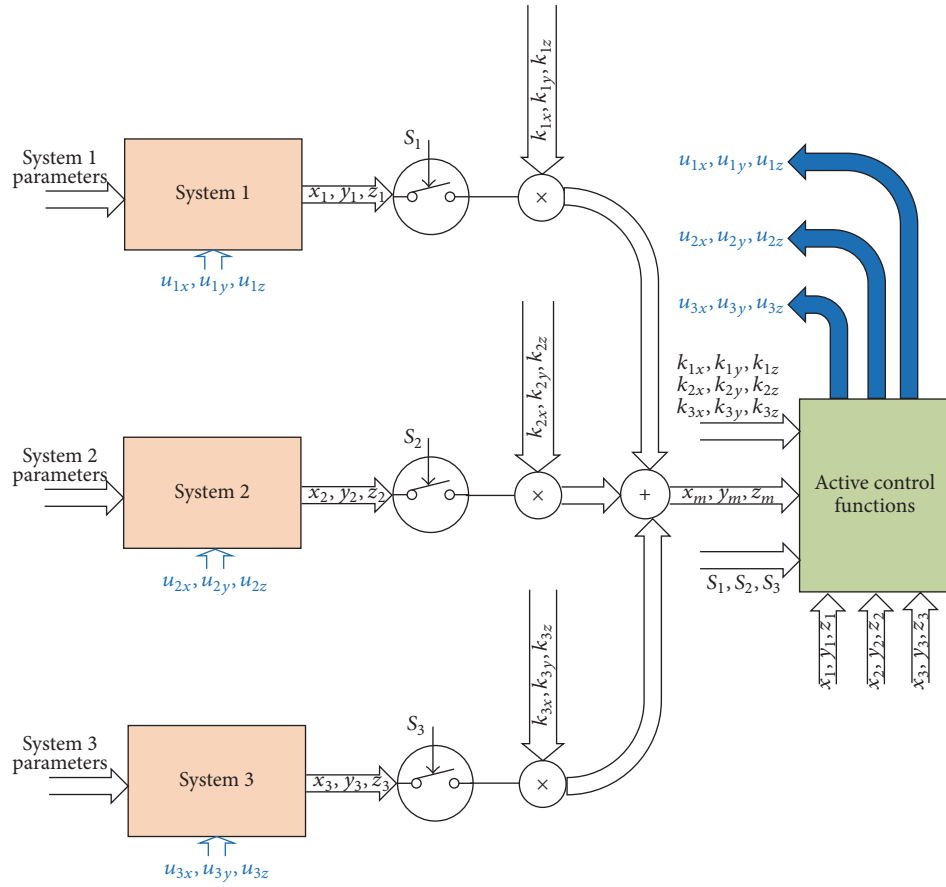


FIGURE 2: Block diagram of the generalized dynamic switched synchronization of three fractional-order chaotic systems.

4. Simulation Results

This section presents several examples to cover the different synchronization capabilities, which are offered by the proposed scheme.

4.1. Static Switching. Static switching is the case in which the role of the system as master or slave is fixed. That is, the control switches (S_i), $i \in \{1, 2, 3\}$, of the systems are time-independent constant values throughout the simulation time.

4.1.1. Single Master. In this case, only one system is allowed to act as a master with the corresponding control switch set to zero. Synchronization could be achieved successfully starting at different initial points. Table 2 shows different cases where only one system acts as a master and the other two systems act as slaves. Colored attractor diagrams show that the synchronization between master-slaves is achieved. In addition, error plots are given, which show that errors decay quickly to zero for the time series of the three phase space dimensions.

4.1.2. Master System Is a Linear Combination. In this case, two of the systems act as a combined master; that is,

the corresponding control switches are set to zero, while the remaining system i is the slave with a control switch that equals one. A novel chaotic response is formed as a “linear” combination of two fractional-order systems and another system is synchronized with this linear combination. Figures 3 and 4 show examples of the constructed linear combinations, colored in dark blue, in which the coefficients k_{ix} , k_{iy} , and k_{iz} are constant throughout the simulation time. These two examples illustrate the path of the systems responses in part of the complete block diagram in Figure 2. The resulting attractor diagram of the slave system is also shown to follow the same trajectory as the master system. In Figure 3(a), CNN and Liu systems are linearly combined to form the resultant master by setting their switches to 0. The resultant master looks similar to Liu as the chosen coefficients of the Liu system (0.8) are greater than those of the CNN system (0.1). Figure 3(b) shows the strange attractor of Financial system, which took the role of a slave by setting its switch to 1. Figure 3(c) shows the time series of the resultant master and slave components, which indicate that the slave system is well synchronized with the resultant master. Figure 4(a) can be described similarly where the resultant master looks similar to Financial system. Figures 4(b) and 4(c) show that the slave system is well synchronized with the resultant master. This linear combination represents

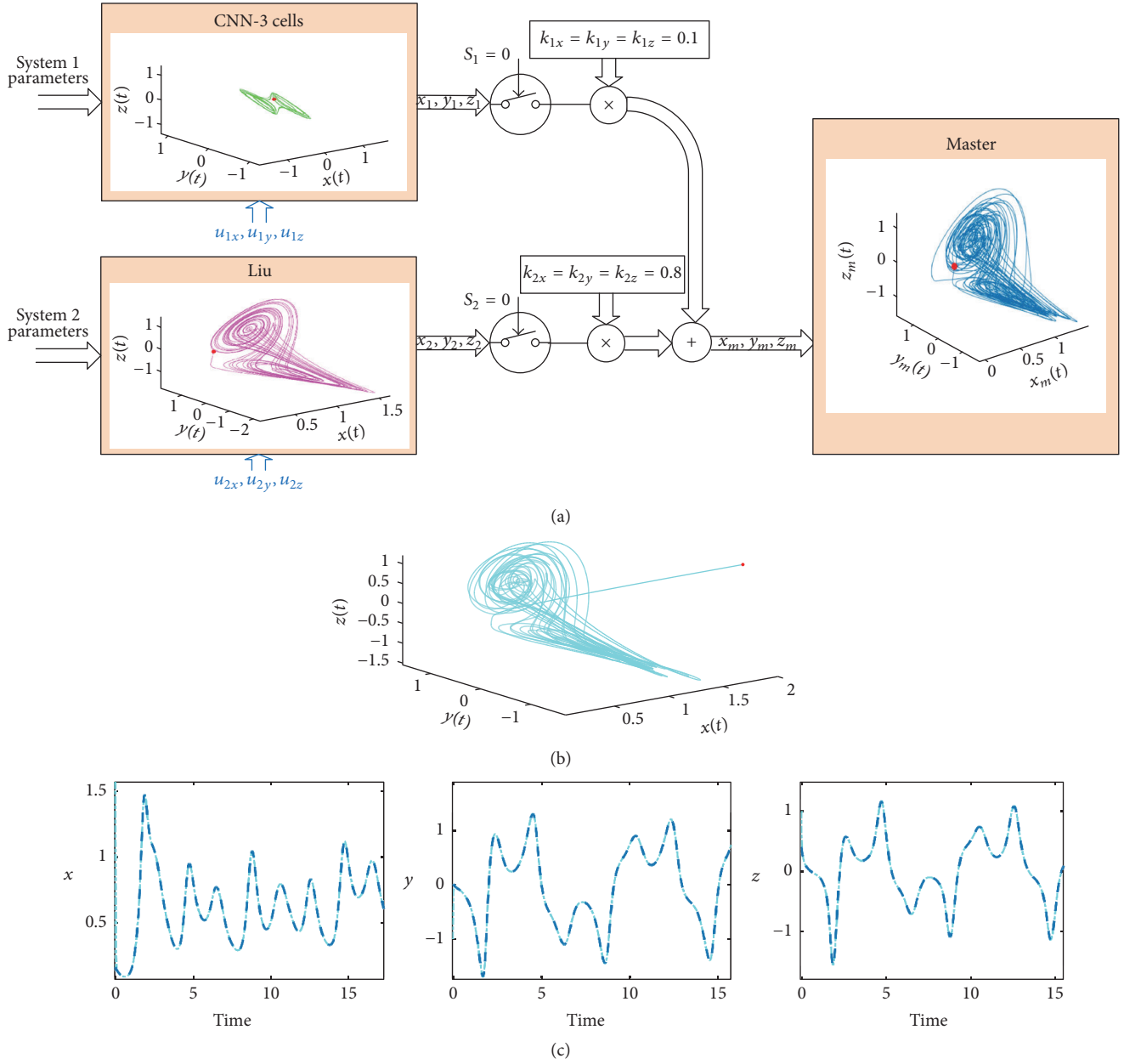
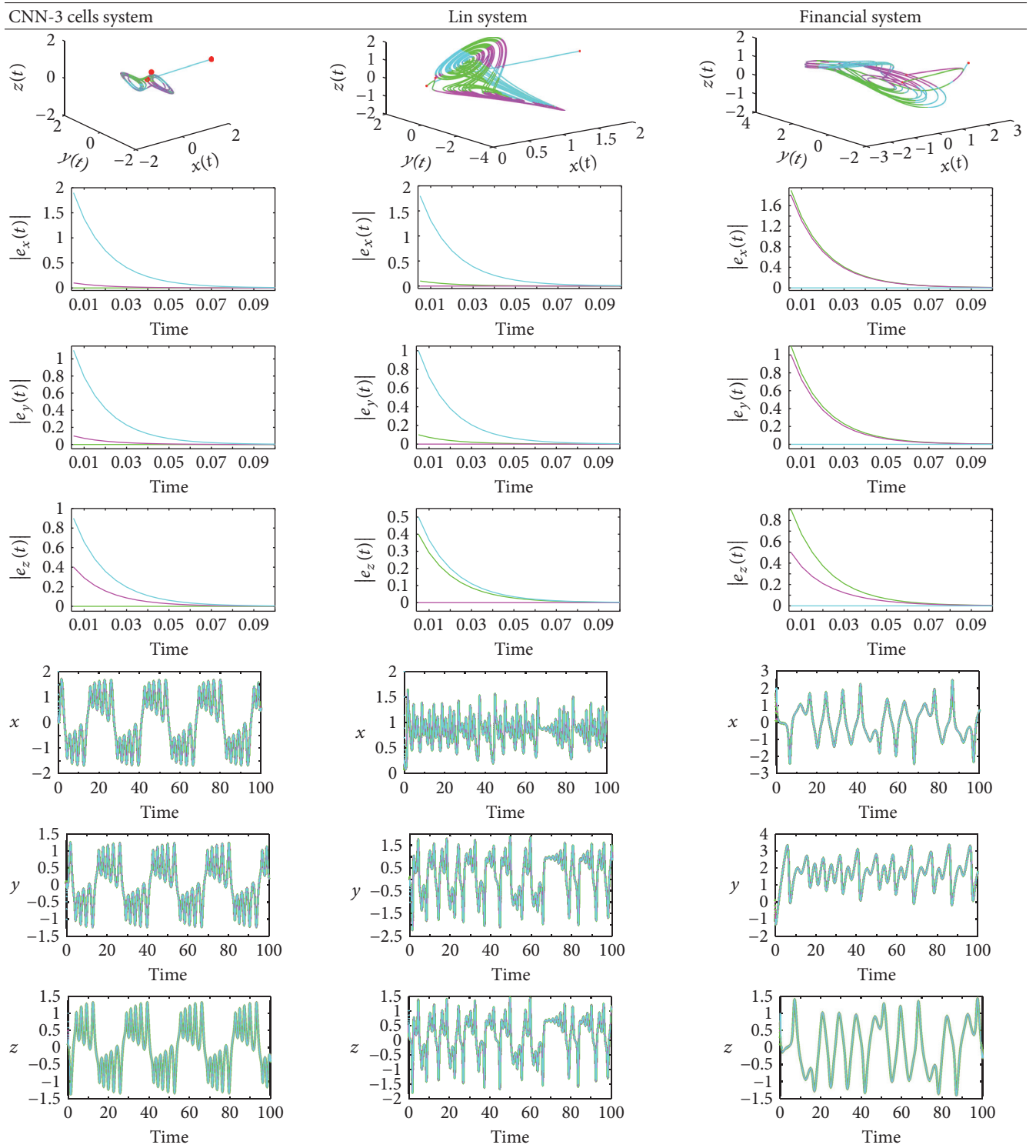


FIGURE 3: (a) Construction of the linear combination of CNN-3 cells and Liu systems with $k_{1x} = k_{1y} = k_{1z} = 0.1$ and $k_{2x} = k_{2y} = k_{2z} = 0.8$, (b) attractor of the slave system successfully synchronized, and (c) time series of both master and slave systems successfully synchronized.

another means of controlling the system response and forcing it to yield the required behavior with more degrees of freedom and controlling capability offered by the coefficients of the linear combination. Table 3 lists further examples of linear combinations formed by each pair of the utilized systems and the corresponding values of scaling factors. In each case, the attractor diagrams of the resultant master and the slave system are successfully synchronized. When the utilized systems have close ranges of outputs, the resulting attractor diagram tends to be similar to that of the system which has a higher value for the coefficient, or weight.

4.2. Dynamic Switching. In this case, the used systems can exchange roles as master or slave throughout the simulation time according to the specified intervals. The example shown in Figure 5 first sets CNN-3 cells as the master system, and then Liu system becomes the master, followed by Financial system. Each system becomes a master for one-third of the total simulation time while the two other systems act as slaves in each time interval. The scaling factors corresponding to each system are set to ones when it acts as a master. The attractor diagram of the master system is shown in Figure 5(a), while Figures 5(b)–5(d) show the attractors of

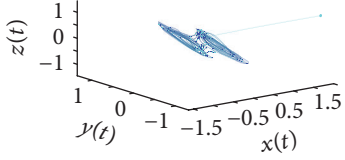
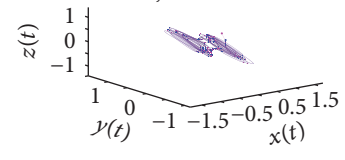
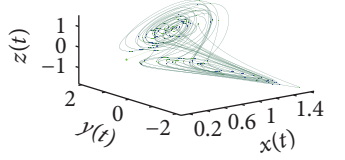
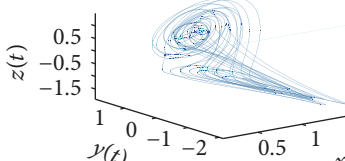
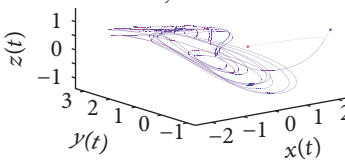
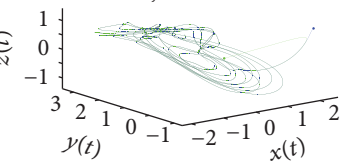
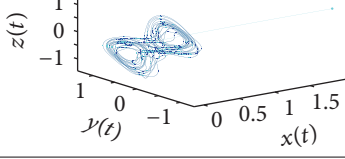
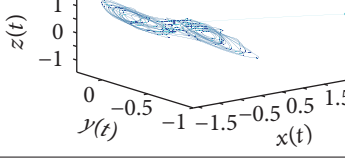
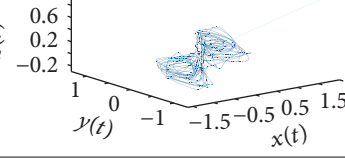
TABLE 2: Attractor diagrams and error functions in case of static synchronization with a single master.



the three systems after synchronization following the same color code in Table 1 and Figure 1 for clarity. The green color corresponds to the first interval of time (following CNN-3 cells), magenta color corresponds to the second interval (following Liu), and cyan color corresponds to the third interval (following Financial system). The red dot shows the initial

point at which each attractor starts. Moreover, Figure 5(e) shows the three time series successfully synchronized with the corresponding values of switches. Various other cases can be discussed similarly where dynamic switching may also be achieved between a linear combination of two systems and the third system.

TABLE 3: Different successfully synchronized linear combinations of the selected systems.

<p>CNN-3 cells & Liu</p> $k_{1x} = k_{1y} = k_{1z} = 1$ $k_{2x} = k_{2y} = k_{2z} = 0.1$ 	<p>CNN-3 cells & Financial</p> $k_{1x} = k_{1y} = k_{1z} = 1$ $k_{3x} = k_{3y} = k_{3z} = 0.1$ 	<p>Liu & Financial</p> $k_{2x} = k_{2y} = k_{2z} = 1$ $k_{3x} = k_{3y} = k_{3z} = 0.1$ 
<p>CNN-3 cells & Liu</p> $k_{1x} = k_{1y} = k_{1z} = 0.1$ $k_{2x} = k_{2y} = k_{2z} = 1$ 	<p>CNN-3 cells & Financial</p> $k_{1x} = k_{1y} = k_{1z} = 0.1$ $k_{3x} = k_{3y} = k_{3z} = 1$ 	<p>Liu & Financial</p> $k_{2x} = k_{2y} = k_{2z} = 0.1$ $k_{3x} = k_{3y} = k_{3z} = 1$ 
<p>CNN-3 cells & Liu</p> $k_{1x} = 0.1, k_{1y} = k_{1z} = 1$ $k_{2x} = k_{2y} = k_{2z} = 0.1$ 	<p>CNN-3 cells & Liu</p> $k_{1x} = k_{1z} = 1, k_{1y} = 0.1$ $k_{2x} = k_{2y} = k_{2z} = 0.1$ 	<p>CNN-3 cells & Liu</p> $k_{1x} = k_{1y} = 1, k_{1z} = 0.1$ $k_{2x} = k_{2y} = k_{2z} = 0.1$ 

4.3. Static and Dynamic Scaling Factors. The scaling factors that are used to construct the master from original system(s) can be constants (static) or functions of time (dynamic). Examples that illustrate the difference between the two cases are shown in Figure 6 and described in detail as follows.

4.3.1. Static Scaling Factors. In this case, each k_{ix} , k_{iy} , and k_{iz} , $i \in \{1, 2, 3\}$, are constant time-independent values. The master responses (x_m , y_m , and z_m) are scaled versions of the original system with the same factor or each with a different factor. The slave system always follows the master system; yet, different relations exist between them and the original system. For positive scaling factor of a given phase space dimension, the slave time series is in-phase (synchronized) with that of the original system. For negative scaling factors, they have an opposite phase (antisynchronized). Moreover, when their absolute values are greater than one, the slave response has a higher amplitude than the original system response, whereas it has a lower amplitude when their absolute values are less than one. Figure 7 shows an example in which Liu is the master system while Financial system and CNN-3 cells are slaves. x time series is scaled by $k_{2x} = -1$, y time series by $k_{2y} = -0.5$, and z time series by $k_{2z} = 2$, which are the same scaling factors of Figure 6(a). Figures 7(a)–7(c) show the time series of the original system which is then scaled with the corresponding scaling factor to get the required master response. That is, x time series of the

master response, and consequently the slave responses, are antisynchronized versions of the original x -time series of Liu system. Their y and z time series equal that of the original Liu system multiplied by -0.5 and 2 , respectively. In addition, the time series of the master and slave responses are successfully synchronized and their attractor diagrams are coincident as shown in Figure 7(d).

4.3.2. Dynamic Scaling Factors. Dynamic scaling represents a generalization with static scaling as a special case. In dynamic scaling, the scaling factors are functions of time as their value(s) could change at each time instant. It could be required that the original and slave systems be in-phase for an interval of the simulation time and then have opposite phase for another interval and so on; that is, the relation between them varies with time in a dynamic manner. In this case, scaling factors need to have some piecewise definition such as $f_{pw}(t) = (-c)^{\text{int}(t/q)}$, where c, q are constants and $\text{int}(\cdot)$ returns the quotient of integer division. This function changes its sign every q time units, more detailed as

$$f_{pw}(t) = (-c)^{\text{int}(t/q)}$$

$$= \begin{cases} c & 2aq \leq t < (2a+1)q \\ -c & (2a+1)q \leq t < (2a+2)q, \end{cases} \quad (15)$$

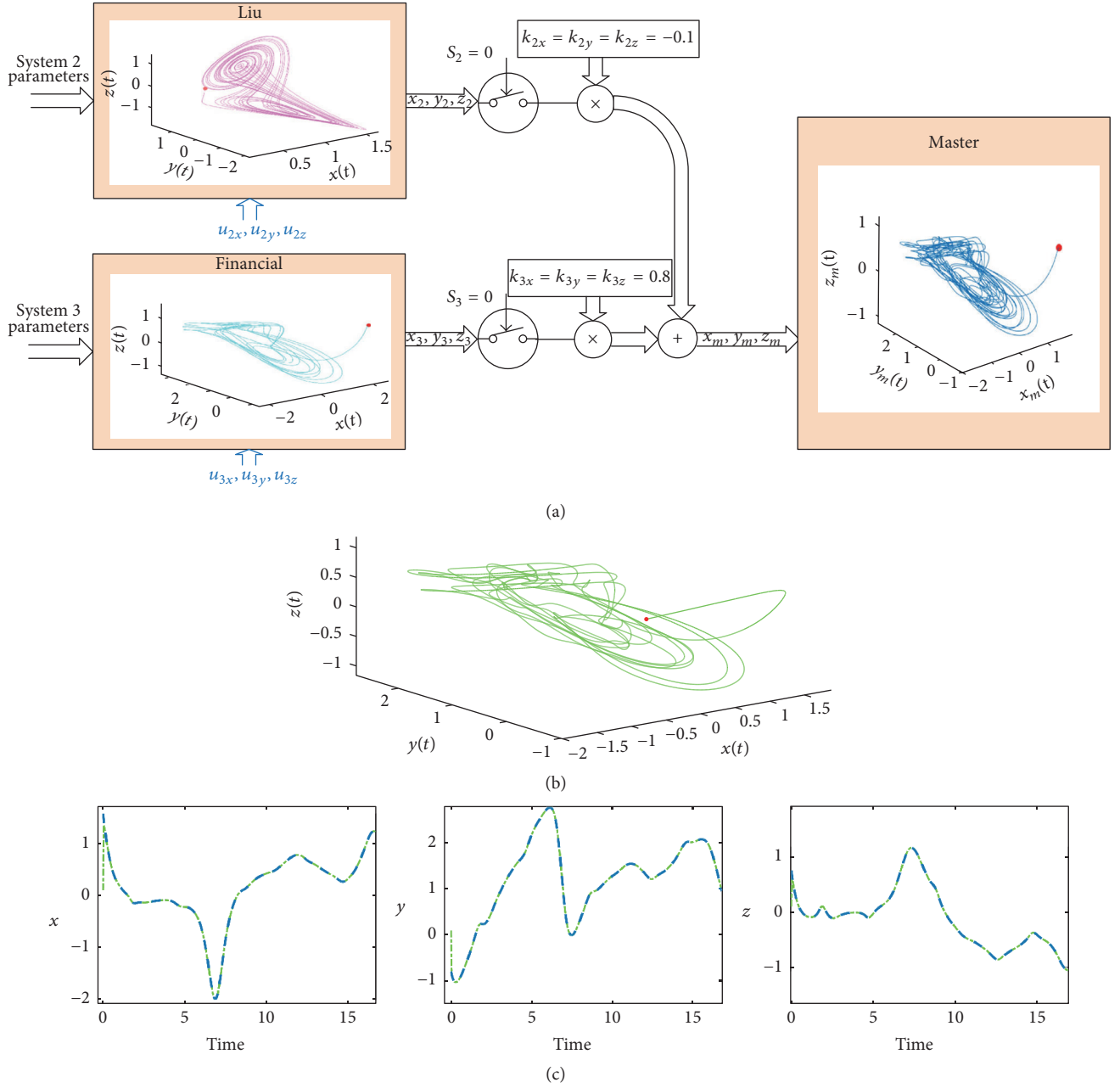


FIGURE 4: (a) Construction of the linear combination of Liu and Financial systems with $k_{2x} = k_{2y} = k_{2z} = -0.1$ and $k_{3x} = k_{3y} = k_{3z} = 0.8$, (b) attractor of the slave system successfully synchronized, and (c) time series of both master and slave systems successfully synchronized.

where a is an integer value. The scaling factor k_x plotted in Figure 6(b) shows an example of $f_{pw}(t)$. Moreover, there are multiple other cases in which k_{ix} , k_{iy} , and k_{iz} , $i \in \{1, 2, 3\}$, could be functions of time. For example, a scaling factor may equal $f_{sc}(t) = c + \text{int}(t/q)$, where c, q are constants and $\text{int}(\cdot)$ returns the quotient of integer division. This is a stair-case function which performs scaling in a variable manner as time advances. The type of synchronization (antisynchronization) and/or its scale changes every q time units as shown in the plot of k_y in Figure 6(b). Another example is $f_{pr}(t) = c + (\text{mod}(t/q))/q$, where c, q are constants and $\text{mod}(\cdot)$ returns

the remainder of integer division. This is a periodic ramp function which is time-dependent too. The value of the scaling factor starts at the value c , and then it increases within every interval of q time units until it resets to c at the end of each interval. The scaling factor k_z plotted in Figure 6(b) shows an example of $f_{pr}(t)$. Other examples, employing more complicated functions, can be applied similarly.

Figure 8 shows an example of generalized dynamic switching synchronization in which Liu is set as the master system for half the time, and then Financial system becomes the master where CNN-3 cells are the slave during all

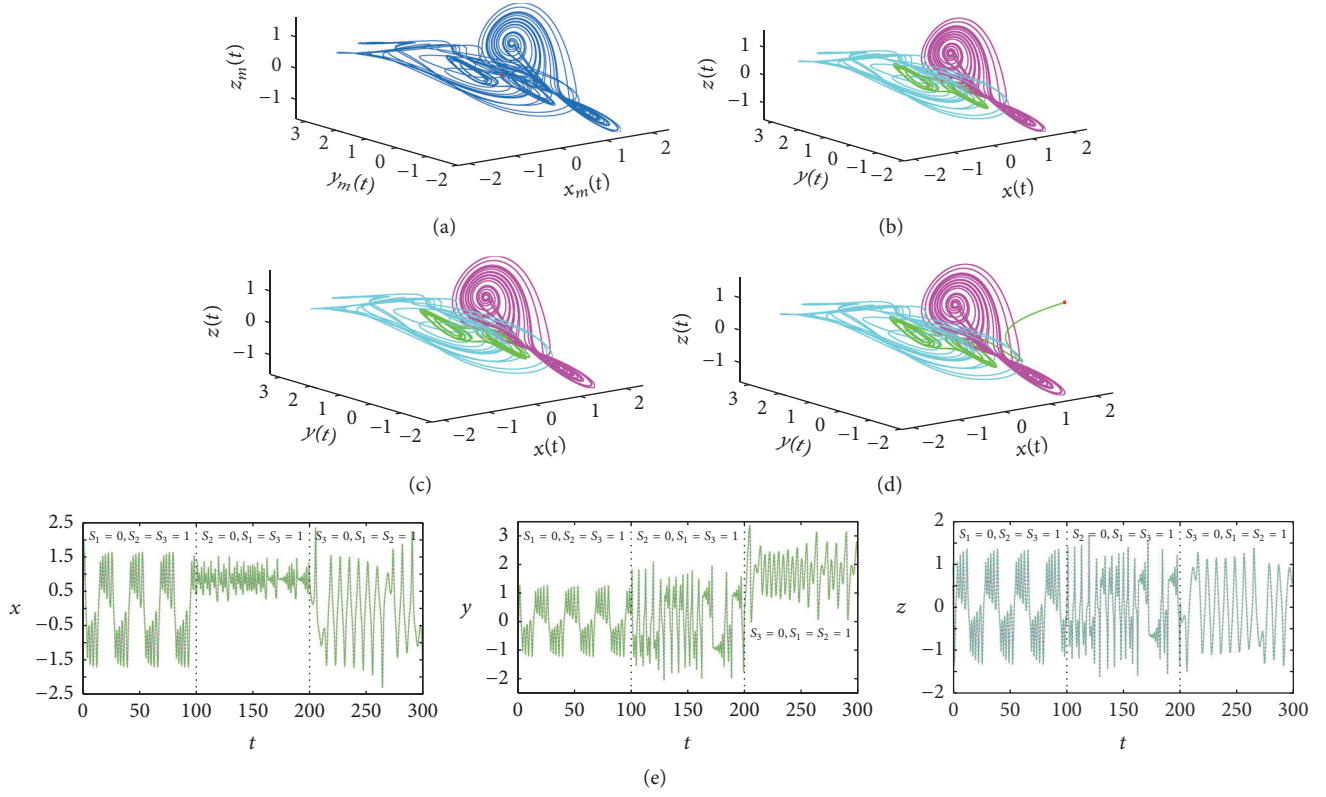


FIGURE 5: Attractors of (a) the master system when switching from CNN-3 cells to Liu then to Financial system as a master each for one-third of the simulation time and the resulting new (b) CNN-3 cells, (c) Liu, (d) Financial systems, and (e) time series successfully synchronized.

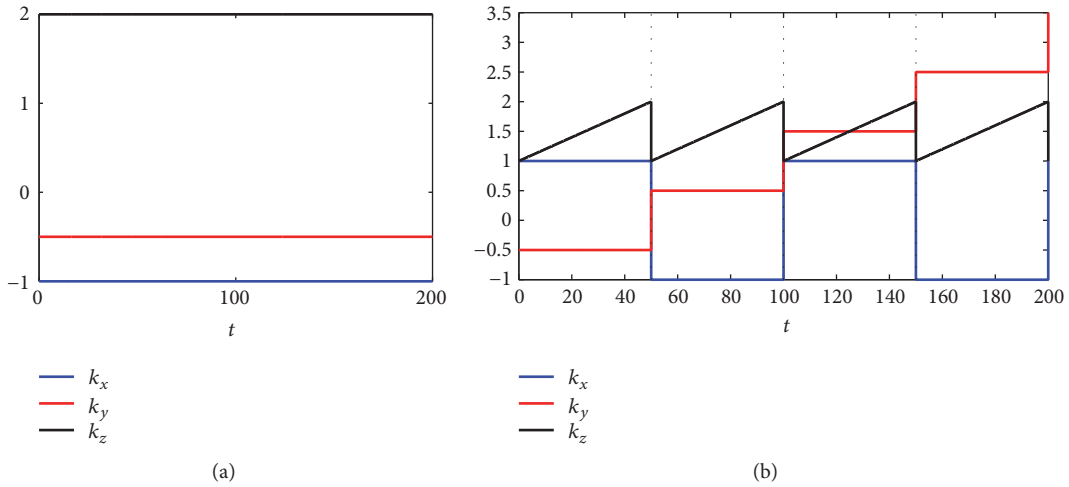


FIGURE 6: (a) Static scaling factors $k_x = -1$, $k_y = -0.5$, and $k_z = 2$ and (b) dynamic scaling factors $k_x = (-1)^{\text{int}(t/50)}$, $k_y = -0.5 + \text{int}(t/50)$, and $k_z = 1 + (\text{mod}(t/50))/50$ versus time.

simulation time. Scaling functions similar to those shown in Figure 6(b) are used, but with different values of total simulation time and q , where x time series is scaled by $k_{2x} = (-1)^{\text{int}(t/10)}$ for $0 \leq t \leq 20$ and $k_{3x} = (-1)^{\text{int}(t/10)}$ for $20 \leq t \leq 40$. y time series is scaled by $-0.5 + \text{int}(t/10)$, and z time series is scaled by $1 + (\text{mod}(t/10))/10$. Each plot

in Figures 8(a)–8(c) shows the time series of the original system which is then scaled to get the master response according to the previously explained behavior of the selected scaling functions. The values of the scaling functions in each interval of time are shown on the plots and the obtained time series follow them precisely. The master and slave responses

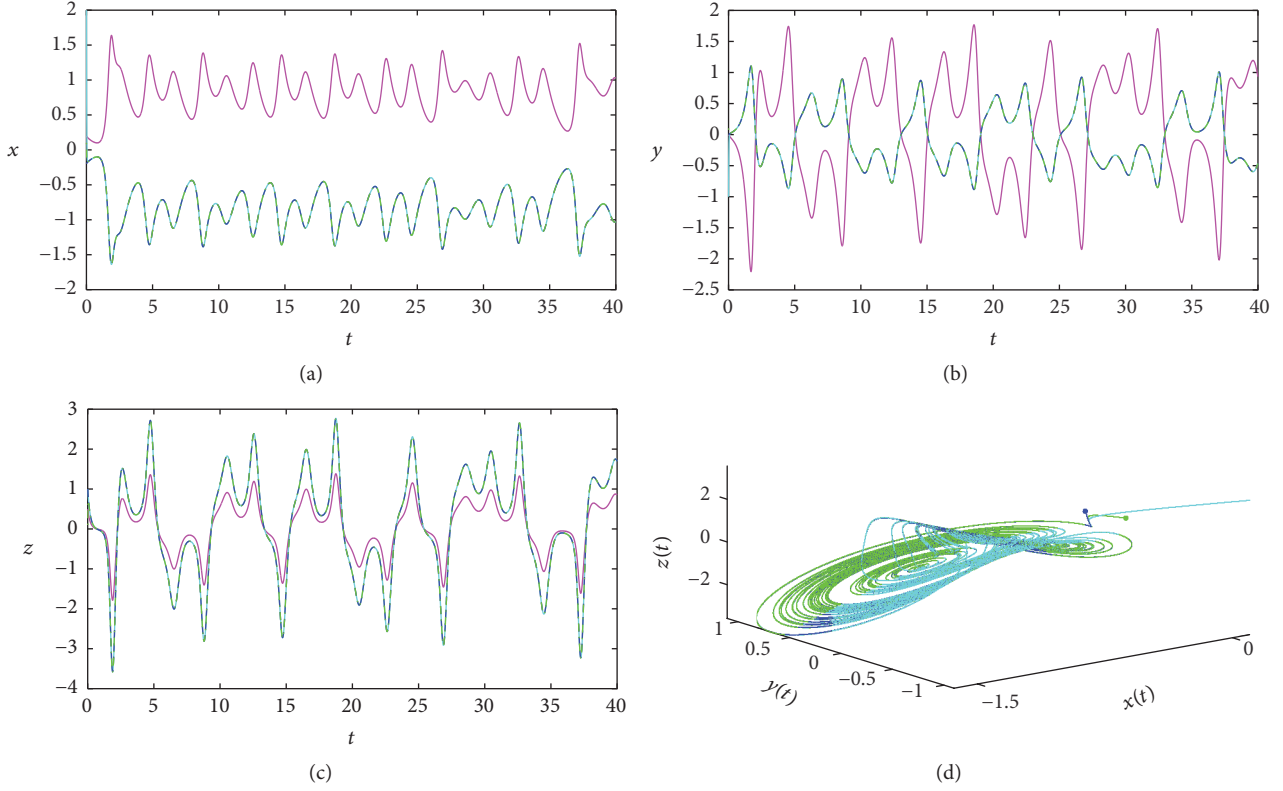


FIGURE 7: Single master synchronization with static scaling factors with Liu system as master and the two other systems as slaves: (a) x time series where $k_{2x} = -1$, (b) y time series where $k_{2y} = -0.5$, (c) z time series where $k_{2z} = 2$, and (d) resulting master and slave systems successfully synchronized.

are successfully synchronized as further illustrated by the coincident attractor diagrams shown in Figure 8(d). Similar results can be obtained for other combinations of the systems and types of synchronization detailed earlier.

From the shape of the attractor diagram shown in Figure 8(d), it is noticed that the scaling factors can be used to get new chaotic trajectories with time series and attractors different from the well-known ones. Table 4 shows some examples illustrating the differences between the attractors of the original systems and those of the newly formed ones. It can, thus, be inferred that dynamic scaling can generate different replicas of the attractor on the same diagram enabling wider output ranges. The attractor diagrams constructed from scaled time series exhibit new shapes of strange attractors with interesting behaviors. Hence, they can be formulated and studied as novel chaotic systems.

5. Discussion and Suggested Applications

In the previous section, simulation results were obtained at $(\alpha, \beta, \gamma) = (0.99, 0.99, 0.99)$ as stated in Section 2. The reason for this choice of the values of fractional orders is that the three utilized systems were shown to exhibit chaotic behavior

at this value. This is suitable for our purpose of demonstrating chaotic synchronization and dynamic switching cases where each system acts as a master for an interval of time. However, the generalized mathematical analysis carried out in Section 3 can be applied for different values of the fractional orders. The effect of the fractional orders on the responses of the three utilized systems has been briefly presented in [63–65] and can be studied through simulations following the experimental approach used in [36, 46]. Table 5 provides several synchronization examples at $(\alpha, \beta, \gamma) = (0.95, 0.92, 0.9)$ and $(\alpha, \beta, \gamma) = (1, 0.93, 0.87)$. The responses of master system and slave system(s) are shown in case of single master static switching synchronization, where CNN-3 cells, Liu, and Financial systems act as masters, respectively. The system of CNN-3 cells exhibits stable response at these values of the fractional orders, while the other two systems remain chaotic. The phase plots show that the master and slaves responses are successfully synchronized irrespective of the response type of the master system. Successful synchronization can also be achieved for the other operation modes including linear combination, dynamic switching, and static and dynamic scaling factors.

These results illustrate another advantage of the proposed synchronization scheme. In addition to changing the chaotic response of the slave system from one form to

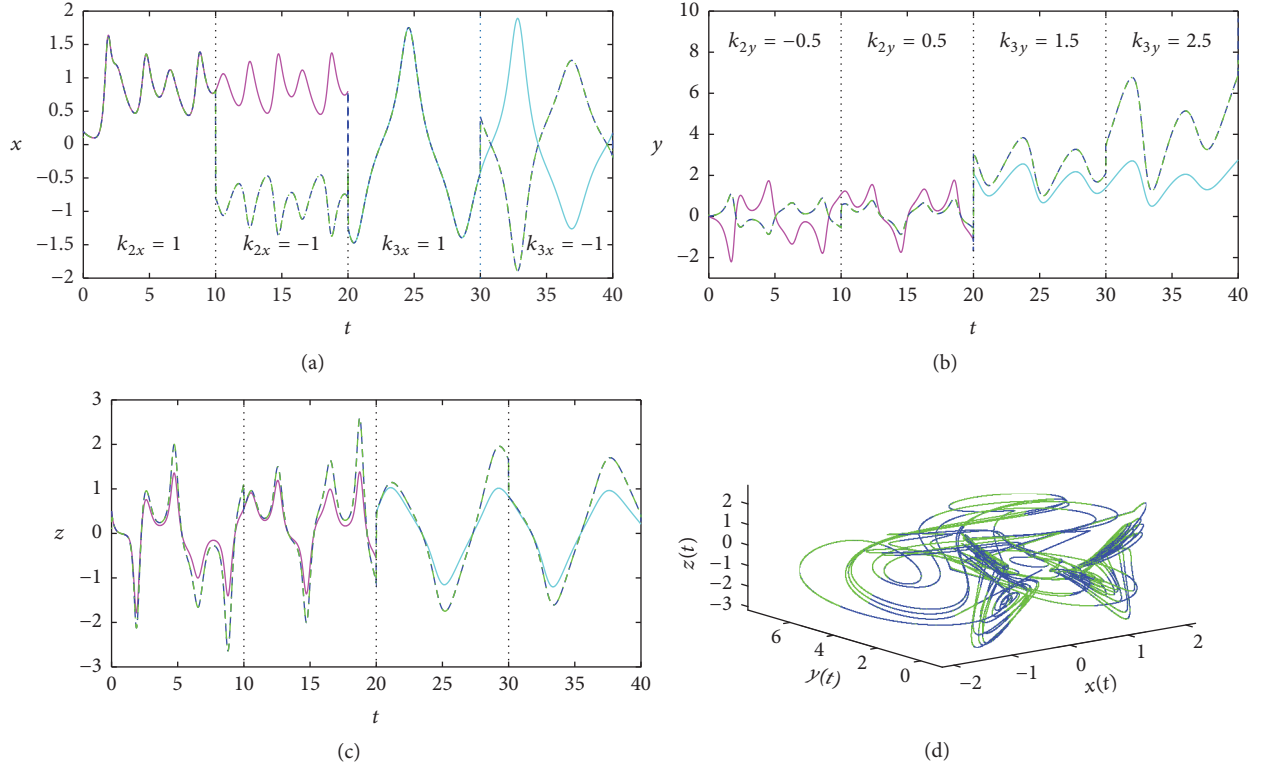


FIGURE 8: Dynamic switched synchronization with dynamic scaling factors: (a) x time series, (b) y time series, (c) z time series, and (d) resulting master and slave systems successfully synchronized.

another, the scheme has the capability of controlling the response type. Stable or periodic systems can be forced to generate chaotic responses, while chaotic systems can be stabilized.

A more generalized scheme can be designed to allow n systems to have different $(\alpha_i, \beta_i, \gamma_i)$ for each system i , where $i = 1, 2, \dots, n$. Such a case has been proposed in few researches such as [67–69]. However, these synchronization schemes do not possess the scaling and switching capabilities presented in our paper.

Each case of those proposed in Section 4 can be mapped to an operating mode of master-slave communication as discussed in Section 1. This includes one-to-one communication, one-to-many communication, multiple masters, mutual interconnections with forward and backward communication, and role switching.

The introduced scheme can be adapted or interfaced with other specific-purpose control blocks. For example, if it is required to have adaptive switching between two identical standby master systems for fairness or maintenance purposes, an external control signal can be used as follows. System 1 acts as a master by setting $S_1 = 0$ and k_{1x}, k_{1y} , and k_{1z} have the required values while $S_2 = k_{2x} = k_{2y} = k_{2z} = 0$ in order that system 2 does not take place in the synchronization, and vice versa when system 2 acts as a master.

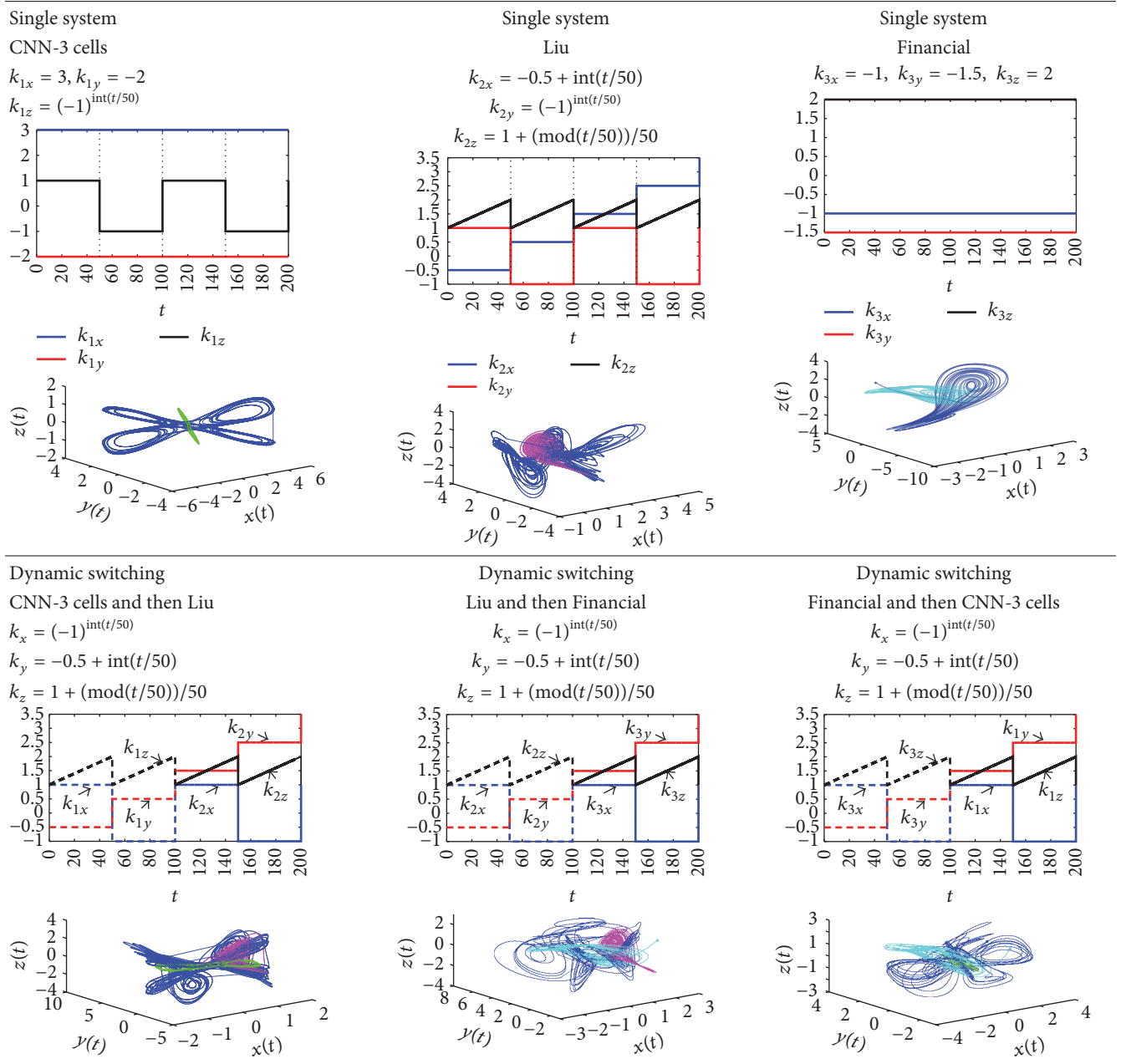
The proposed scheme, which utilizes dynamic scaling factors, can be useful for amplitude modulation applications

in which the amplitude of the output signal should be a function of the input signal. Dynamic scaling factors can play the role of information signal, which is modulated by the chaotic dynamics of the system to give the modulated signal. Demodulation can be done similarly by reversing the operation.

6. Conclusions

In this paper, we have proposed a novel generalized switched synchronization scheme among n fractional-order chaotic systems. The proposed scheme offers various capabilities utilizing a set of dynamic switches and scaling factors. Generalized mathematical analysis permits adapting the switches and scaling factors to perform various functions. The switches control the role of each system as a master or a slave. Each system can either have a fixed role, that is, master or slave, throughout the simulation time, which is called static switching or change its role one or more times in case of dynamic switching. The scaling factors control the generalized relation between the original systems from which the master system is built on the one hand as well as the slave system(s) on the other hand. They can also be static or dynamic according to the required application. Moreover, in all of the presented cases, the master system can be a single system or a combination of

TABLE 4: New attractor diagrams formed by static and dynamic scaling of the original systems.



two or more systems. The proposed scheme can also apply different scaling factors to the time series of each state variable to design new attractor diagrams. Generalized switched synchronization, as presented in this paper, can fit many applications such as master-slave communication models, chaotic amplitude modulation, and secure communication systems.

Future work includes updating the proposed scheme to cover the case where the master and slave components have derivatives of different fractional orders. The proposed

scheme can also be used to develop secure communication systems for multimedia applications including speech, image, and video. Moreover, implementation issues need to be considered in terms of computational complexity and memory requirements. The results obtained for fractional-order chaotic systems including fractional time derivatives can be interpreted in terms of memory. Consequently, the tradeoff between computational efficiency of the proposed generalized synchronization scheme and the required accuracy should be considered in a hardware implementation.

TABLE 5: Successful synchronization at different values of the fractional orders.

Orders	System responses and single master synchronization results		
	CNN	Liu	Financial
$\alpha = 0.95$ $\beta = 0.92$ $\gamma = 0.9$			
$\alpha = 1$ $\beta = 0.93$ $\gamma = 0.87$			

Competing Interests

The authors declare that there is no conflict of interests regarding the publication of this paper.

References

- [1] D. R. Frey, "Chaotic digital encoding: an approach to secure communication," *IEEE Transactions on Circuits and Systems II: Analog and Digital Signal Processing*, vol. 40, no. 10, pp. 660–666, 1993.
- [2] F. Lau and C. K. Tse, *Chaos-Based Digital Communication Systems*, Springer, Berlin, Germany, 2003.
- [3] L. Kocarev and S. Lian, *Chaos-Based Cryptography: Theory, Algorithms and Applications*, vol. 354, Springer, Berlin, Germany, 2011.
- [4] A. G. Radwan and S. K. Abd-El-Hafiz, "Image encryption using generalized tent map," in *Proceedings of the IEEE 20th International Conference on Electronics, Circuits, and Systems (ICECS '13)*, pp. 653–656, IEEE, Abu Dhabi, UAE, December 2013.
- [5] A. G. Radwan, S. K. Abd-El-Hafiz, and S. H. Abdelhaleem, "An image encryption system based on generalized discrete maps," in *Proceedings of the 21st IEEE International Conference on Electronics, Circuits and Systems (ICECS '14)*, pp. 283–286, IEEE, Marseille, France, December 2014.
- [6] S. K. Abd-El-Hafiz, A. G. Radwan, and S. H. Abdel-Haleem, "Encryption applications of a generalized chaotic map," *Applied Mathematics & Information Sciences*, vol. 9, no. 6, pp. 1–19, 2015.
- [7] W. S. Sayed, A. G. Radwan, and H. A. H. Fahmy, "Design of positive, negative, and alternating sign generalized logistic maps," *Discrete Dynamics in Nature and Society*, vol. 2015, Article ID 586783, 23 pages, 2015.
- [8] W. S. Sayed, A. G. Radwan, and H. A. H. Fahmy, "Design of a generalized bidirectional tent map suitable for encryption applications," in *Proceedings of the 11th International Computer Engineering Conference (ICENCO '15)*, pp. 207–211, IEEE, Cairo, Egypt, December 2015.
- [9] A. G. Radwan, A. S. Elwakil, and A. M. Soliman, "Fractional-order sinusoidal oscillators: design procedure and practical examples," *IEEE Transactions on Circuits and Systems. I. Regular Papers*, vol. 55, no. 7, pp. 2051–2063, 2008.
- [10] A. G. Radwan, A. M. Soliman, and A. S. Elwakil, "First-order filters generalized to the fractional domain," *Journal of Circuits, Systems, and Computers*, vol. 17, no. 1, pp. 55–66, 2008.
- [11] A. G. Radwan, "Stability analysis of the fractional-order $rl\beta ca$ circuit," *Journal of Fractional Calculus and Applications*, vol. 3, no. 1, pp. 1–15, 2012.
- [12] A. G. Radwan, "Resonance and quality factor of the fractional circuit," *IEEE Journal on Emerging and Selected Topics in Circuits and Systems*, vol. 3, no. 3, pp. 377–385, 2013.
- [13] S. K. Han, C. Kurrer, and Y. Kuramoto, "Dephasing and bursting in coupled neural oscillators," *Physical Review Letters*, vol. 75, no. 17, pp. 3190–3193, 1995.
- [14] E. Schöll, *Nonlinear Spatio-Temporal Dynamics and Chaos in Semiconductors*, vol. 10, Cambridge University Press, 2001.
- [15] S. H. Strogatz, "Nonlinear dynamics and chaos: with applications to physics, biology, chemistry, and engineering," Westview Press, 2014.
- [16] R. Gorenflo and F. Mainardi, *Fractional Calculus*, Springer, Berlin, Germany, 1997.
- [17] R. Caponetto, *Fractional Order Systems: Modeling and Control Applications*, vol. 72, World Scientific, 2010.
- [18] R. L. Magin, *Fractional Calculus in Bioengineering*, Begell House Redding, 2006.
- [19] A. G. Radwan, A. Shamim, and K. N. Salama, "Theory of fractional order elements based impedance matching networks," *IEEE Microwave and Wireless Components Letters*, vol. 21, no. 3, pp. 120–122, 2011.
- [20] A. Shamim, A. G. Radwan, and K. N. Salama, "Fractional smith chart theory," *IEEE Microwave and Wireless Components Letters*, vol. 21, no. 3, pp. 117–119, 2011.
- [21] A. G. Radwan, S. K. Abd-El-Hafiz, and S. H. Abdelhaleem, "Image encryption in the fractional-order domain," in *Proceedings of the 1st International Conference on Engineering and Technology (ICET '12)*, 6, 1 pages, October 2012.
- [22] M.-C. Ho and Y.-C. Hung, "Synchronization of two different systems by using generalized active control," *Physics Letters A*, vol. 301, no. 5–6, pp. 424–428, 2002.
- [23] T.-I. Chien and T.-L. Liao, "Design of secure digital communication systems using chaotic modulation, cryptography and chaotic synchronization," *Chaos, Solitons & Fractals*, vol. 24, no. 1, pp. 241–255, 2005.

- [24] S. Bhalekar and V. Daftardar-Gejji, "Synchronization of different fractional order chaotic systems using active control," *Communications in Nonlinear Science and Numerical Simulation*, vol. 15, no. 11, pp. 3536–3546, 2010.
- [25] X. Wu, H. Wang, and H. Lu, "Modified generalized projective synchronization of a new fractional-order hyperchaotic system and its application to secure communication," *Nonlinear Analysis: Real World Applications*, vol. 13, no. 3, pp. 1441–1450, 2012.
- [26] L.-G. Yuan and Q.-G. Yang, "Parameter identification and synchronization of fractional-order chaotic systems," *Communications in Nonlinear Science and Numerical Simulation*, vol. 17, no. 1, pp. 305–316, 2012.
- [27] M. R. Faieghi and H. Delavari, "Chaos in fractional-order Genesio-Tesi system and its synchronization," *Communications in Nonlinear Science and Numerical Simulation*, vol. 17, no. 2, pp. 731–741, 2012.
- [28] S. K. Agrawal, M. Srivastava, and S. Das, "Synchronization of fractional order chaotic systems using active control method," *Chaos, Solitons & Fractals*, vol. 45, no. 6, pp. 737–752, 2012.
- [29] D. Chen, R. Zhang, X. Ma, and S. Liu, "Chaotic synchronization and anti-synchronization for a novel class of multiple chaotic systems via a sliding mode control scheme," *Nonlinear Dynamics. An International Journal of Nonlinear Dynamics and Chaos in Engineering Systems*, vol. 69, no. 1-2, pp. 35–55, 2012.
- [30] D. Chen, C. Wu, H. H. C. Iu, and X. Ma, "Circuit simulation for synchronization of a fractional-order and integer-order chaotic system," *Nonlinear Dynamics*, vol. 73, no. 3, pp. 1671–1686, 2013.
- [31] M. Srivastava, S. P. Ansari, S. K. Agrawal, S. Das, and A. Y. Leung, "Anti-synchronization between identical and non-identical fractional-order chaotic systems using active control method," *Nonlinear Dynamics. An International Journal of Nonlinear Dynamics and Chaos in Engineering Systems*, vol. 76, no. 2, pp. 905–914, 2014.
- [32] M.-C. Ho, Y.-C. Hung, and C.-H. Chou, "Phase and anti-phase synchronization of two chaotic systems by using active control," *Physics Letters A: General, Atomic and Solid State Physics*, vol. 296, no. 1, pp. 43–48, 2002.
- [33] M. T. Yassen, "Chaos synchronization between two different chaotic systems using active control," *Chaos, Solitons & Fractals*, vol. 23, no. 1, pp. 131–140, 2005.
- [34] K. Moaddy, A. G. Radwan, K. N. Salama, S. Momani, and I. Hashim, "The fractional-order modeling and synchronization of electrically coupled neuron systems," *Computers & Mathematics with Applications*, vol. 64, no. 10, pp. 3329–3339, 2012.
- [35] A. G. Radwan, K. Moaddy, and I. Hashim, "Amplitude modulation and synchronization of fractional-order memristor-based Chua's circuit," *Abstract and Applied Analysis*, vol. 2013, Article ID 758676, 10 pages, 2013.
- [36] A. G. Radwan, K. Moaddy, K. N. Salama, S. Momani, and I. Hashim, "Control and switching synchronization of fractional order chaotic systems using active control technique," *Journal of Advanced Research*, vol. 5, no. 1, pp. 125–132, 2014.
- [37] L. M. Pecora and T. L. Carroll, "Synchronization in chaotic systems," *Physical Review Letters*, vol. 64, no. 8, pp. 821–824, 1990.
- [38] S. S. Yang and C. K. Duan, "Generalized synchronization in chaotic systems," *Chaos, Solitons & Fractals*, vol. 9, no. 10, pp. 1703–1707, 1998.
- [39] T. Yang and L. O. Chua, "Generalized synchronization of chaos via linear transformations," *International Journal of Bifurcation and Chaos*, vol. 9, no. 1, pp. 215–219, 1999.
- [40] M. Juan and W. Xingyuan, "Generalized synchronization via nonlinear control," *Chaos*, vol. 18, no. 2, Article ID 023108, 2008.
- [41] M. P. Aghababa, "Control of non-integer-order dynamical systems using sliding mode scheme," *Complexity*, vol. 21, no. 6, pp. 224–233, 2016.
- [42] K. Mathiyalagan, J. H. Park, and R. Sakthivel, "Exponential synchronization for fractional-order chaotic systems with mixed uncertainties," *Complexity*, vol. 21, no. 1, pp. 114–125, 2015.
- [43] C. Yin, Y. Cheng, S.-M. Zhong, and Z. Bai, "Fractional-order switching type control law design for adaptive sliding mode technique of 3D fractional-order nonlinear systems," *Complexity*, vol. 21, no. 6, pp. 363–373, 2016.
- [44] R. Behinfaraz and M. Badamchizadeh, "Optimal synchronization of two different in-commensurate fractional-order chaotic systems with fractional cost function," *Complexity*, vol. 21, no. S1, pp. 401–416, 2016.
- [45] W. S. Sayed, A. G. Radwan, and S. K. Abd-El-Hafiz, "Generalized synchronization involving a linear combination of fractional-order chaotic systems," in *Proceedings of the 13th International Conference on Electrical Engineering/Electronics, Computer, Telecommunications and Information Technology (ECTI-CON '16)*, pp. 1–6, IEEE, Chiang Mai, Thailand, 2016.
- [46] M. M. R. Henein, W. S. Sayed, A. G. Radwan, and S. K. Abd-El-Hafiz, "Switched active control synchronization of three fractional order chaotic systems," in *Proceedings of the IEEE 13th International Conference on Electrical Engineering/Electronics, Computer, Telecommunications and Information Technology (ECTI-CON '16)*, pp. 1–6, 2016.
- [47] A. Frotzsch, U. Wetzker, M. Bauer et al., "Requirements and current solutions of wireless communication in industrial automation," in *Proceedings of the IEEE International Conference on Communications Workshops (ICC '14)*, pp. 67–72, IEEE, Sydney, Australia, June 2014.
- [48] Y. Yang, J. Wu, X. Sun, J. Wu, and C. Zheng, "Development and application of a master-slave parallel hybrid multi-objective evolutionary algorithm for groundwater remediation design," *Environmental Earth Sciences*, vol. 70, no. 6, pp. 2481–2494, 2013.
- [49] M. Mitsuishi, A. Morita, N. Sugita et al., "Master-slave robotic platform and its feasibility study for micro-neurosurgery," *International Journal of Medical Robotics and Computer Assisted Surgery*, vol. 9, no. 2, pp. 180–189, 2013.
- [50] Z. Li and C.-Y. Su, "Neural-adaptive control of single-master-multiple-slaves teleoperation for coordinated multiple mobile manipulators with time-varying communication delays and input uncertainties," *IEEE Transactions on Neural Networks and Learning Systems*, vol. 24, no. 9, pp. 1400–1413, 2013.
- [51] M. Ashjaei, M. Behnam, T. Nolte, and L. Almeida, "Performance analysis of master-slave multi-hop switched ethernet networks," in *Proceedings of the 8th IEEE International Symposium on Industrial Embedded Systems (SIES '13)*, pp. 280–289, June 2013.
- [52] M. Ashjaei, P. Pedreiras, M. Behnam, L. Almeida, and T. Nolte, "Evaluation of dynamic reconfiguration architecture in multi-hop switched ethernet networks," in *Proceedings of the 19th IEEE International Conference on Emerging Technologies and Factory Automation (ETFA '14)*, 65, 62 pages, September 2014.
- [53] S. Mastellone, D. Lee, and M. W. Spong, "Master-slave synchronization with switching communication through passive model-based control design," in *Proceedings of the 2006 American Control Conference*, IEEE, Minneapolis, Minn, USA, 2006.
- [54] S. Trifunovic, A. Picu, T. Hossmann, and K. A. Hummel, "Slicing the battery pie: fair and efficient energy usage in device-to-device communication via role switching," in *Proceedings*

- of the 8th ACM MobiCom Workshop on Challenged Networks (CHANTS '13), pp. 31–36, Miami, Florida, USA, September 2013.
- [55] S. Trifunovic, A. Picu, T. Hossmann, and K. A. Hummel, "Adaptive role switching for fair and efficient battery usage in device-to-device communication," *ACM SIGMOBILE Mobile Computing and Communications Review*, vol. 18, no. 1, pp. 25–36, 2014.
 - [56] M. S. El Moursi, H. H. Zeineldin, J. L. Kirtley Jr., and K. Alobeidli, "A dynamic master/slave reactive power-management scheme for smart grids with distributed generation," *IEEE Transactions on Power Delivery*, vol. 29, no. 3, pp. 1157–1167, 2014.
 - [57] D. Lin, X. Wang, F. Zhang, and Y. Yao, "Mutual synchronization behavior for chaotic systems via limited capacity communication channels," *Complexity*, vol. 21, no. 6, pp. 335–342, 2016.
 - [58] I. Petras, *Fractional-Order Nonlinear Systems: Modeling, Analysis and Simulation*, Springer Science & Business Media, 2011.
 - [59] I. Podlubny, *Fractional Differential Equations: An Introduction to Fractional Derivatives, Fractional Differential Equations, to Methods of Their Solution and Some of Their Applications*, vol. 198, Academic Press, 1998.
 - [60] E. F. Doungmo Goufo, "Stability and convergence analysis of a variable order replicator-mutator process in a moving medium," *Journal of Theoretical Biology*, vol. 403, pp. 178–187, 2016.
 - [61] E. F. Doungmo Goufo, "Chaotic processes using the two-parameter derivative with non-singular and non-local kernel: basic theory and applications," *Chaos. An Interdisciplinary Journal of Nonlinear Science*, vol. 26, no. 8, 2016.
 - [62] E. F. D. Goufo, "Application of the Caputo-Fabrizio fractional derivative without singular kernel to Korteweg-de Vries-Burgers equation," *Mathematical Modelling and Analysis*, vol. 21, no. 2, pp. 188–198, 2016.
 - [63] P. Arena, R. Caponetto, L. Fortuna, and D. Porto, "Bifurcation and chaos in noninteger order cellular neural networks," *International Journal of Bifurcation and Chaos*, vol. 8, no. 7, pp. 1527–1539, 1998.
 - [64] V. Daftardar-Gejji and S. Bhalekar, "Chaos in fractional ordered Liu system," *Computers & Mathematics with Applications*, vol. 59, no. 3, pp. 1117–1127, 2010.
 - [65] W.-C. Chen, "Nonlinear dynamics and chaos in a fractional-order financial system," *Chaos, Solitons and Fractals*, vol. 36, no. 5, pp. 1305–1314, 2008.
 - [66] A. G. Radwan, K. Moaddy, and S. Momani, "Stability and non-standard finite difference method of the generalized Chua's circuit," *Computers & Mathematics with Applications*, vol. 62, no. 3, pp. 961–970, 2011.
 - [67] Z. M. Odibat, "Adaptive feedback control and synchronization of non-identical chaotic fractional order systems," *Nonlinear Dynamics. An International Journal of Nonlinear Dynamics and Chaos in Engineering Systems*, vol. 60, no. 4, pp. 479–487, 2010.
 - [68] P. Zhou and W. Zhu, "Function projective synchronization for fractional-order chaotic systems," *Nonlinear Analysis: Real World Applications*, vol. 12, no. 2, pp. 811–816, 2011.
 - [69] G. Si, Z. Sun, Y. Zhang, and W. Chen, "Projective synchronization of different fractional-order chaotic systems with non-identical orders," *Nonlinear Analysis. Real World Applications. An International Multidisciplinary Journal*, vol. 13, no. 4, pp. 1761–1771, 2012.

